

gTLO: A Generalized and Non-linear Multi-Objective Deep Reinforcement Learning Approach

Johannes Dornheim

Abstract—In real-world decision optimization, often multiple competing objectives must be taken into account. Following classical reinforcement learning, these objectives have to be combined into a single reward function. In contrast, multi-objective reinforcement learning (MORL) methods learn from vectors of per-objective rewards instead. In the case of multi-policy MORL, sets of decision policies for various preferences regarding the conflicting objectives are optimized. This is especially important when target preferences are not known during training or when preferences change dynamically during application. While it is, in general, straightforward to extend a single-objective reinforcement learning method for MORL based on linear scalarization, solutions that are reachable by these methods are limited to convex regions of the Pareto front. Non-linear MORL methods like Thresholded Lexicographic Ordering (TLO) are designed to overcome this limitation. Generalized MORL methods utilize function approximation to generalize across objective preferences and thereby implicitly learn multiple policies in a data-efficient manner, even for complex decision problems with high-dimensional or continuous state spaces. In this work, we propose *generalized Thresholded Lexicographic Ordering* (gTLO), a novel method that aims to combine non-linear MORL with the advantages of generalized MORL. We introduce a deep reinforcement learning realization of the algorithm and present promising results on a standard benchmark for non-linear MORL and a real-world application from the domain of manufacturing process control.

Index Terms—Multi-Objective Reinforcement Learning, Multi-objective decision making, Deep Reinforcement Learning.

I. INTRODUCTION

IN real-world decision problems, decisions often result from balancing multiple objectives. In pure, single objective, reinforcement learning, the objectives are reflected by a single scalar reward function where the optimal decision is chosen to maximize the expected future reward [1]. If the objectives are not in alignment, the optimal decision is typically not clearly definable. Instead, the decision depends on scenario-specific preferences, e.g. the relative importance of each objective. Therefore, multi-objective reinforcement learning (MORL) is based on a setting in which the scalar reward function is replaced by a vector-valued reward function. This allows the design of reinforcement learning agents, which consider the various objectives during decision-making [2]. In contrast to *single-policy* MORL algorithms which use the reward vectors

to optimize a specific policy for explicitly or implicitly defined objective preferences, *multi-policy* MORL algorithms learn a set of preference-dependent optimal policies [3]. This is especially useful in scenarios in which the online preferences are not known during agent training [4]. This includes the *dynamic preferences* scenario [5], where the preferences are non-stationary during application. This scenario is given for example in domains in which the optimization criteria depend on dynamic prices of open markets [4], or on changing requirements for process results [6].

In this work, we focus on *multi-policy* MORL methods, which themselves can be classified into *outer loop* methods and *inner loop* methods [7]. Outer loop methods decompose the multi-policy problem into a series of problems with defined preferences, that are solved by a single-policy approach. Inner loop methods, on the other hand, are designed to solve the multi-policy optimization problem without the need for an outer loop. A recent and broad review of MORL methods can be found in [8].

One branch of inner loop MORL methods, which we name *generalized* MORL, is to learn expected value functions that generalize over objective preferences [9]–[13]. Contrary to approaches where separate value functions are learned independently per preference, these *generalized* MORL methods can transfer knowledge about the decision problem in between different preferences. The first published method that falls into this category is *Multi-Objective Fitted Q-Iteration* (MOFQ) by Castelletti et al. [9], a generalized MORL variant of *Fitted Q-iteration* [14] based on regression trees. Friedman et al. [11] took up this idea by extending *Deep Deterministic Policy Gradients* [15] and *Hindsight Experience Replay* [16] to a generalized deep MORL method for continuous applications. Abels et al. [10] proposed a generalized deep method based on generalized vector-valued *Q-functions*, approximated by a weight-conditioned network (CN). They proposed *Diverse Experience Replay* for sample efficient learning and to avoid catastrophic forgetting in the dynamic preferences setting. Yang et al. [12] proposed *Envelope Q-learning* (EQL) based on a generalized form of the Bellman update equation that utilizes the convex envelope of the solution frontier for linear approaches. Tajmajer [13] proposed a method that can also be classified as generalized MORL, but differs from the already mentioned by introducing additional and dynamic per-state weights, which are called *decision values*, and by learning an independent Deep Q-Network (DQN) [17] model per objective. *Decision values* are learned by the agent as part

Johannes Dornheim is with the Institute for Applied Materials - Computational Materials Science (IAM - CMS), Karlsruhe Institute of Technology, Germany and the Intelligent Systems Research Group (ISRG), Karlsruhe University of Applied Sciences, Germany (e-mail: johannes.dornheim@mailbox.org).

of the extended DQNs and bind the preferences to the agent’s state.

The ability of generalized MORL methods to efficiently optimize multiple preference-dependent policies has been shown in several publications, examples are [9], [10]. Castelletti et al. [9] showed that the sample efficiency of MOFQ compared to an *outer loop* baseline rapidly increases with the number of policies for different preferences considered and already exceeds the baseline when more than five preferences are considered. A key result of the comparative study in [10] is, that the proposed generalized MORL approach outperforms a state of the art outer loop approach based on [18] and [5] in terms of sample efficiency.

Although current methods for generalized MORL are sample efficient, they combined preference values with expected values in a linear manner to derive decisions or to learn expected value functions. When observed in the space of per-objective expected returns, linear methods can identify policies that belong to expected returns from the *convex coverage set*, which is a subset of the *Pareto coverage set* [2], [19]. In practice, this limitation can lead to (i) agent behavior that is sub-optimal concerning the preference at hand, (ii) situations where balanced solutions are not found [20] and (iii) situations where small changes in the preference values cause huge changes in the policy [3]. Non-linear MORL methods aim to overcome this problem. Basic approaches for non-linear MORL include non-linear scalarization [21], the explicit storing and pruning of sets of non-dominated Q-vectors [22], [23] and objective thresholding [3], [24], [25]. While early algorithms for non-linear MORL [3], [21], [23], [24], [26] are based on tabular reinforcement learning, more recent methods [25], [27], [28] are based on deep reinforcement learning and are therefore also applicable in real-world applications with high-dimensional and often continuous state descriptions. The *Pareto DQN* [27] is a deep MORL version of the *Pareto Q-Learning* (PQL) algorithm [22]. It aims to directly approximate the Pareto front and, to the best of our knowledge, is the only published approach that aims to solve multi-policy MORL problems in a non-linear and *inner loop* fashion.

Thresholded Lexicographic Ordering (TLO) is a popular non-linear single-policy approach, proposed by Gábor et al. [24] for multi-objective problems, in which one of the reward components has to be optimized, while the other components are constrained by minimum thresholds. Vamplew et al. [3] proposed an alternative implementation of TLO based on vector-valued multi-objective Q-Learning, *Thresholded Lexicographic Q-learning* (TLQ). They showed that TLO / TLQ can be used as the basis of outer loop non-linear multi-policy learning by varying the minimum thresholds between the single-policy optimization runs. TLO / TLQ is applicable as long as the problem is finite-horizon and the reward components, that are subject to constraints are non-zero on terminal states only [3]. Nguyen et al. [25] combined TLQ with DQN for deep reinforcement learning tasks with graphical state representations. Li et al. [28] proposed a single-goal algorithm with adaptive thresholding and Q-function factoring methods for autonomously navigating intersections based on DQN and TLO.

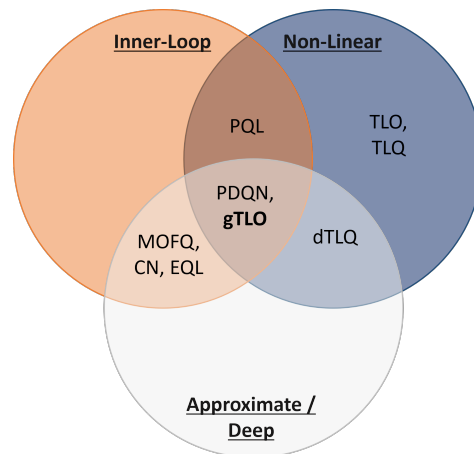


Fig. 1. Grouping of the most related multi-policy MORL-methods discussed above by various aspects represented as a Venn Diagram. Shown are: Thresholded Ordering methods (TLO [24], TLQ [3], *dTLQ* [25]), generalized MORL methods (MOFQ [9], CN [10], EQL [12]), methods that directly approximate the Pareto-front (PQL [22], PDQN [27]) and *gTLO* (ours).

In this paper we present a MORL method that is (a) non-linear, (b) solves multi-policy problems in a generalized and thus inner loop fashion, and (c) can be combined with value-based deep reinforcement learning. The most related of the methods identified and discussed above are grouped by these three aspects in the Venn Diagram in Fig. 1. As discussed above, non-linear methods have the advantage that they are not limited to finding solutions from the *convex coverage set* in general. Current generalized MORL approaches (including MOFQ [9], CN [10], EQL [12]) fall into the linear regime. While tabular methods (e.g. PQL [22], TLO [24] and TLQ [3]) are able to solve small-scale problems, approximate reinforcement learning and deep reinforcement learning enables to scale to real-world problems with high-dimensional or continuous state spaces without suffering the *curse of dimensionality*. Most current non-linear multi-policy methods, including the TLO-based methods (TLO [24], TLQ [3], *dTLQ* [25]), rely on a simple outer loop strategy and determine multiple policies by independently running a single-policy algorithm per preference. While this approach is limited to cases with only a few optimal policies and with knowledge about the location and course of the Pareto front ([3], [25]), inner loop methods enable to scale to more realistic cases with many Pareto-optimal solutions and without knowledge about the location of those. The only published method we found that falls into the inner intersection of the Venn diagram is PDQN [27], which is an “initial attempt” to integrate PQL into deep RL [8]. However, presented results of PDQN indicate that the method in its current form is limited to problems with low-dimensional state spaces and only delivers very raw estimates of the true *Pareto coverage set* [27].

The contribution of our work is threefold:

- 1) We propose *gTLO*: a non-linear generalized MORL method that combines the ability of generalized MORL to learn multiple optimal policies in a sample efficient manner, with the ability of the non-linear MORL method TLO to not being limited to the *convex coverage set*. To

the best of our knowledge *gTLO* is the first non-linear generalized MORL method.

- 2) While *gTLO* is combinable with various value-based reinforcement learning algorithms, we present and evaluate an implementation based on vanilla *Deep Q-networks* (DQN).
- 3) We present a comprehensive evaluation of our algorithm on two environments. First, we use an image-based version of the deep-sea treasure [19] environment, which is a common benchmark, especially for non-linear MORL. Second, we evaluate our method on an environment from the manufacturing context: the multi-objective online optimization of blank holding forces of deep drawing processes [29].

II. BACKGROUND

A. Single Objective Reinforcement Learning

The formal basis of reinforcement learning (RL) is the Markov decision process (MDP) [1]. MDPs are described by the tuple (S, A, R, γ, P) , where actions $a \in A$ lead from a Markovian state $s \in S$ to a subsequent state $s' \in S$, following the state transition probability function $P(s'|s, a)$. A reward value $r \in \mathbb{R}$ is given to the agent during the transition from s to s' , following the reward function $R(s, a, s')$. In some processes, especially in the case of infinite-horizon MDPs, future rewards are discounted by a discount factor $\gamma \in [0, 1]$. We limit ourselves to finite-horizon MDPs within this work, where special absorbing states $\bar{S} \subset S$ exist. One sequence of decisions leading from a starting state s_0 to one of the absorbing states \bar{S} is called an episode. Reinforcement learning methods aim to learn a policy $\pi : S \times A \rightarrow [0, 1]$ during interaction with the process without any given a priori knowledge of P or R . When following π , for any state s the action a is selected according to the probability $\pi(s, a)$. The goal is to learn an optimal policy π^* , which maximizes the expected future rewards collected until an absorbing state is reached by the agent. As usual in value-based RL, we consider deterministic optimal policies $\bar{\pi}^*$ ¹. We denote deterministic policies by $\bar{\pi}$ throughout the paper and define it as a direct mapping from states to actions $\bar{\pi} : S \rightarrow A$.

In value-based reinforcement learning, functions of expected, possibly discounted, future rewards are learned. The Q -function is such a function and is defined for any policy π on state-action tuples by

$$Q_\pi(s, a) = \mathbb{E}_{P, \pi} [R(s, a, s') + \gamma Q_\pi(s', a')]. \quad (1)$$

The Q -function of an optimal policy $\bar{\pi}^*$ is denoted by $Q^* = Q_{\bar{\pi}^*}$. In Q-learning [31], Q^* is learned by iteratively applying the Bellman Q -function update

$$Q(s, a) \leftarrow Q(s, a) + \alpha \tau \quad (2)$$

¹When R is bounded, A is finite and if at least one optimal policy exists for the MDP, it is guaranteed that at least one deterministic optimal policy $\bar{\pi}^*$ exists for that MDP (compare [30], Ch. 6). For multi-objective MDPs (MOMDP), scenarios exist where stochastic policies can dominate deterministic policies [2]. In the case of a finite horizon, this can be prevented by extending the MOMDPs state space.

based on experience tuples (s, a, s', r) , where

$$\tau := r + \gamma \max_{a' \in A} Q(s', a') - Q(s, a) \quad (3)$$

is the so called *temporal difference error*. For online learning, experience tuples are collected during process interaction by following an explorative policy π_ϵ . As long as for all actions $a \in A$ and states $s \in S$ it is true that $\pi_\epsilon(s, a) > 0$, the estimation Q is guaranteed to converge to Q^* [1]. Once Q^* is given, an optimal deterministic policy can be easily extracted: $\bar{\pi}^*(s) = \arg \max_{a \in A} Q^*(s, a)$.

Pure Q-learning relies on an $\mathbb{R}^{|S| \times |A|}$ matrix to store the Q -value estimations, thus it suffers the *curse of dimensionality* regarding the state space dimensions and can only be applied to discrete state spaces. In real-world applications, where a state s is often described by a real-valued vector $\mathbf{s} \in \mathbb{R}^n$ or matrix, function approximation is used to overcome the problems of tabular learning. In value-based deep reinforcement learning, approaches are typically based on the *Deep Q-Networks* algorithm (DQN) [17]. In DQN, the Q -function is approximated by a neural network $\mathcal{Q} \approx Q$. The approximation is usually implemented as $\mathcal{Q}(\mathbf{s}, \theta)$, where \mathbf{s} is a description of the state s , θ are the network parameters and $\mathcal{Q}(\mathbf{s}, \theta)_i$ approximates $Q(s, a_i)$, where actions are indexed by i . For the sake of simplicity, we instead use the notation $\mathcal{Q}(\mathbf{s}, a, \theta) \approx Q(s, a)$ throughout the paper.

Experience-tuples are stored in a so-called *replay memory*, from which mini-batches of experiences are uniformly sampled for parameter updates. The training target for an experience tuple (s, a, s', r) is then

$$y_{\mathcal{Q}} \leftarrow r + \gamma \max_{a' \in A} \mathcal{Q}(s', a', \theta^-), \quad (4)$$

where the *target-parameters* θ^- are decoupled from the continuously updated *online-parameters* θ , that are used to form the explorative policy π_ϵ (and thereby influence the distribution of sampled experience tuples) to stabilize learning. Every n_θ time steps the target-parameters are updated by replacement $\theta^- \leftarrow \theta$.

B. Multi-Objective Reinforcement Learning

In many decision optimization problems, instead of a single objective, multiple objectives have to be optimized simultaneously. These problems can be formalized as multi-objective Markov decision processes [2] (MOMDPs) $(S, A, P, \mathcal{R}, \gamma)$. Instead of scalar rewards, $\mathcal{R}(s, a, s')$ emits a reward vector $\mathbf{r} \in \mathbb{R}^I$, where each component reflects one of the I objectives. The system dynamics are described by Markov states $s \in S$, actions $a \in A$, and the transition probability function P as in the standard MDP. In typical MOMDPs, the objectives are not in alignment, and instead of a single policy that solves the process, the optimal policy depends on the importance of each objective, according to the users, or the application-dependent preference. Multi-objective reinforcement learning (MORL) methods differ in how these preferences are expressed.

One can quantify the expected multi-objective return of each policy when starting in state s on time step t by defining a vector-valued multi-objective state-value function

$$\mathbf{V}_\pi(s) = \mathbb{E}_{P,\pi} \left[\sum_{k=t}^{\infty} \gamma^k \mathbf{r}_{k+1} \right], \quad (5)$$

where for the considered case of finite-horizon MDPs all rewards are zero ($\mathbf{r} = \mathbf{0}$) after the end of the episode. When considering a finite-horizon MOMDP with a fixed starting-state s_0 , the expected multi-objective return per episode is given by $\mathbf{V}_\pi(s_0)$, which we denote by \mathbf{V}_π . Policies π that are optimal for any trade-off between the objectives are part of the so-called *Pareto front*. A policy $\pi \in \Pi$ is part of the Pareto front if it is not dominated by any other policy $\pi' \in \Pi \setminus \pi$ through the *Pareto dominance relation* ($\forall i : \mathbf{V}_{\pi',i} \geq \mathbf{V}_{\pi,i} \wedge (\exists i : \mathbf{V}_{\pi',i} > \mathbf{V}_{\pi,i})$) for $1 \leq i \leq I$, where Π is the set of executable policies. While various policies π on the Pareto front may have the same expected return value \mathbf{V}_π , one is typically only interested in a single policy per value. A so-called *Pareto coverage set* (PCS) as desired solution set, therefore, is a subset of the Pareto front and consists of one policy per undominated value [2].

In MORL, preferences for I objectives are often expressed by parameters $\mathbf{w} \in \mathbb{R}^I$ of a scalarization function $f(\mathbf{r}, \mathbf{w})$ and the goal is to maximize the *scalarized expected return* $f(\mathbf{V}_\pi(s), \mathbf{w})$. Due to its simplicity, usual choice for scalarization is the weighted sum

$$f_s(\mathbf{r}, \mathbf{w}) = \sum_{i \in [1, m]} \mathbf{r}_i \mathbf{w}_i, \quad (6)$$

which is additive ($f_s(\mathbf{r}, \mathbf{w}) + f_s(\mathbf{r}', \mathbf{w}) = f_s(\mathbf{r} + \mathbf{r}', \mathbf{w})$) and the *scalarized expected return* (SER) equals the *expected scalarized return* (ESR)

$$f_s \left(\mathbb{E}_{P,\pi} \left[\sum_{k=t}^{\infty} \gamma^k \mathbf{r}_{k+1} \right], \mathbf{w} \right) = \mathbb{E}_{P,\pi} \left[\sum_{k=t}^{\infty} \gamma^k f_s(\mathbf{r}_{k+1}, \mathbf{w}) \right]. \quad (7)$$

According to this property, linear scalarization is easily combine-able with conventional value-based reinforcement learning methods. In the most basic case, Q-learning can be used to learn the action-dependent ESR [32].

Also, existing *generalized MORL* methods are based on linear scalarization. Generalization across preference-vectors \mathbf{w} is realized either

- by learning a generalized function of the *expected scalarized return* (ESR) $\mathcal{Q}(s, a, \mathbf{w}, \theta) \approx Q_{\mathbf{w}}(s, a_i)$ [9], [11], where $Q_{\mathbf{w}}$ is the Q function for $f_s(\bullet, \mathbf{w})$, or
- by learning a vector-valued Q-function $\mathcal{Q}(s, a, \mathbf{w}, \theta) \approx \mathbf{Q}(s, a, \mathbf{w})$, where $\mathbf{Q}(s, a, \mathbf{w})_i$ is the expected future reward for objective i and preference \mathbf{w} , and scalarizing it (SER) for policy-extraction [10], [12].

Policies that are optimal w.r.t. f_s for any preference-vector \mathbf{w} form the *convex coverage set* (CCS), which is a subset of the *Pareto coverage set* [2], [19]. The CCS includes only policies π , where the expected return \mathbf{V}_π is located in a convex region of the Pareto front. Consequently, linear MORL is limited to

identifying PCS policies with expected returns in non-convex regions, and thereby incomplete [3], [20]. This motivates the research of non-linear approaches.

Unlike linear scalarization, non-linear scalarization functions are not additive and the *scalarized expected return* (SER) in general, differs from the *expected scalarized return* (ESR) [8], [20]. The additivity of reward sequences is a basic assumption of the Bellman update. As this is not the case for sequences of non-linearly scalarized rewards, policies that are optimal under ESR learning, (i.e. following $\max_a \mathcal{Q}(s, a, \mathbf{w}, \theta)$), in general, differ from policies that are optimal under the SER criterion (i.e. following $\max_a f(\mathcal{Q}(s, a, \mathbf{w}, \theta))$). The objective in multi-objective optimization is typically to maximize the *scalarized expected return* (SER) $f(E(s_0))$ and to find the *Pareto coverage set*².

C. Thresholded Lexicographic Ordering

Instead of a *scalarization function*, Thresholded Lexicographic Ordering (TLO) [24] is based on a non-linear action selection mechanism. Preferences are given in the form of minimum thresholds $\mathbf{t} = (t_0, \dots, t_I)^\top$ for the I reward components ($\mathbf{r} \in \mathbb{R}^I$). The last objective is unconstrained, thus formally $t_I = +\infty$. TLO aims to select an action that maximizes \mathbf{Q}_I , while the minimum constraints $\mathbf{Q}_i > t_i$ are met for $i \in [0, I - 1]$. During learning, the action selection mechanism guides the agent to gradually find policies that fulfill the threshold constraints. The action a^* is selected by TLO in state s , if the superior-proposition $\text{sup}(a^*, a, s, 0)$ is true for every $a \in A \setminus a^*$ [3]. Based on a thresholded Q-function

$$\mathbf{Q}\mathbf{t}(s, a)_i = \min(\mathbf{Q}(s, a)_i, t_i), \quad (8)$$

the superior-proposition is defined by

$$\begin{aligned} \text{sup}(a^*, a, s, i) := & \mathbf{Q}\mathbf{t}(s, a^*)_i > \mathbf{Q}\mathbf{t}(s, a)_i \vee \\ & [\mathbf{Q}\mathbf{t}(s, a^*)_i = \mathbf{Q}\mathbf{t}(s, a)_i \wedge (i = I \vee \text{sup}(a^*, a, s, i + 1))]. \end{aligned} \quad (9)$$

The TLO policy $\bar{\pi}_{\text{TLO}}$ then assigns the associated TLO action a^* to each state s . A noisy version of $\bar{\pi}_{\text{TLO}}$ is used during learning for exploration.

In the original TLO approach [24], the thresholded form of the Q-function $\mathbf{Q}\mathbf{t}(s, a)$ is learned, by applying value iteration updates to it directly. This potentially leads to massively biased estimations of $\mathbf{Q}\mathbf{t}(s, a)$, especially when TLO is combined with function approximation [28]. In the modified TLO version named TLQ [3], instead, the vector-valued \mathbf{Q} function is learned, and $\mathbf{Q}\mathbf{t}$ is calculated based on \mathbf{Q} during action selection. For learning \mathbf{Q} , the standard Q-learning update is applied independently per objective

$$\mathbf{Q}(s, a)_i \leftarrow \mathbf{Q}(s, a)_i + \alpha [\mathbf{r}_i + \gamma_i \max_{a' \in A} \mathbf{Q}(s', a')_i - \mathbf{Q}(s, a)_i]. \quad (10)$$

²There are cases in which the maximization of *expected scalarized returns* is more suitable [2]. This case is covered in recent work [33].

This off-policy update is based on the assumption that the best subsequent action a' is chosen to maximize the current objective i independently from other objectives. In [28], Li et al. also propose to learn \mathbf{Q} , but avoid the mentioned problems by taking the TLO action selection into account during the update.

III. gTLO: GENERALIZED THRESHOLDED LEXICOGRAPHIC ORDERING

As in other generalized MORL approaches, we aim to learn a Q-function $\mathbf{Q}(s, a, \mathbf{w}, \theta)$ that generalizes over preference parameters \mathbf{w} , where in our case instead of linear scalarization the TLO action selection mechanism is applied. Therefore, in our case, the preference parameters \mathbf{w} are the TLO threshold values \mathbf{t} , and $\mathbf{Q}(s, a, \mathbf{t})_i$ denotes the expected reward r_i for reward-component i under the condition, that the agent fulfills the threshold constraints. In contrast to other TLO based algorithms, where either a single policy for a predefined threshold-vector \mathbf{t} [3], [24] or for an adaptive \mathbf{t} [28] is learned, we learn a generalized Q-function $\mathbf{Q}(s, a, \mathbf{t})$ and thereby a generalized form of the TLO policy $\bar{\pi}_{\text{TLO}}(s, \mathbf{t})$.

To simplify the following description of *gTLO*, we reformulate the TLO action selection mechanism from Section II-C based on sets $\hat{A}_{(\mathbf{t}, i, s)} \subseteq A$ of actions for which the expected future rewards $\mathbf{Q}(s, a, \mathbf{t})_j$ are sufficient regarding the thresholds \mathbf{t}_j up to i for state s

$$\hat{A}_{(\mathbf{t}, i, s)} := \{a \in A \mid \mathbf{Q}(s, a, \mathbf{t})_j > \mathbf{t}_j, \forall j \in [0, i]\}. \quad (11)$$

As shown in detail in appendix A, the deterministic policy $\bar{\pi}_{\text{TLO}}$, which greedily follows the TLO action selection for a threshold-vector \mathbf{t} , can then be expressed by the conditioned argumentum maximi

$$\bar{\pi}_{\text{TLO}} \leftarrow \begin{cases} \arg \max_{a \in A} \mathbf{Q}(s, a, \mathbf{t})_0, & \text{if } |\hat{A}_{(\mathbf{t}, 0, s)}| = 0, \\ \arg \max_{a \in \hat{A}_{(\mathbf{t}, I, s)}} \mathbf{Q}(s, a, \mathbf{t})_I, & \text{if } |\hat{A}_{(\mathbf{t}, I, s)}| > 0, \\ \arg \max_{a \in \hat{A}_{(\mathbf{t}, i, s)}} \mathbf{Q}(s, a, \mathbf{t})_{i+1}, & \text{otherwise,} \end{cases} \quad (12)$$

where in the third case $i := \max_i : |\hat{A}_{(\mathbf{t}, i, s)}| > 0$. In the following, we specify our idea of a generalized Q-function for TLO and then introduce the deep *gTLO* Network.

A. Generalized TLO Q-Function

The direct per-objective off-policy Q-learning update as in (10) implies the assumption that a' is chosen to maximize the current objective independently from other objectives. As shown in (11) and (12), the TLO policy $\bar{\pi}_{\text{TLO}}(s, \mathbf{t})$ chooses a from a set of actions \hat{A}_i , which itself depends on expected reward values $\mathbf{Q}(s, a, \mathbf{t})_j$ for objectives $j < i$. Learning seems to be possible in the single-policy tabular case despite the systematic positive bias resulting from this incorrect assumption as shown in [3]. However, in our case of learning a generalized Q-function with function approximation methods, we observe a massive negative impact of this bias on the learning performance.

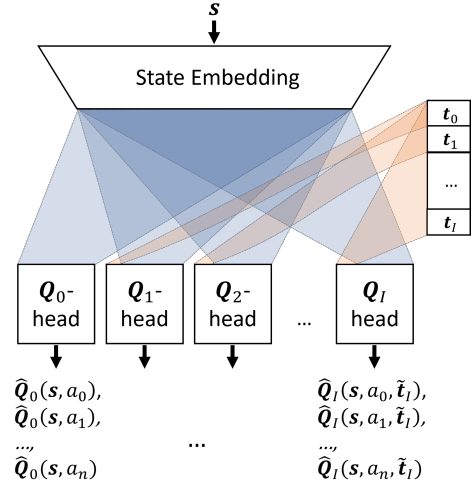


Fig. 2. General model architecture of the generalizedTLO Network

In some tabular methods with vector-valued Q-functions the on-policy SARSA update is used to avoid this problem with the off-policy update [34]. However, value-based deep reinforcement learning in general and generalized MORL in particular heavily rely on historic data for Q-function approximation. In addition to the policy shift, these data may be experienced under outdated preferences. These off-policy data can not be used for on-policy learning. Instead, inspired by [28], where a similar update is proposed for single-policy MORL with adaptive thresholds, we define the Q-function update in a way that considers the TLO action selection mechanism by restricting the set from which the hypothetical follow-up action a' is chosen:

$$\mathbf{Q}(s, a, \mathbf{t})_i \leftarrow \mathbf{Q}(s, a, \mathbf{t})_i + \alpha \tau_{\text{TLO}}, \quad (13)$$

where

$$\tau_{\text{TLO}} := \mathbf{r}_i + \gamma_i \max_{a' \in \tilde{A}_{(\mathbf{t}, i, s')}} \mathbf{Q}(s', a', \mathbf{t})_i - \mathbf{Q}(s, a, \mathbf{t})_i \quad (14)$$

is a special form of the *temporal difference error*, which is based on the restricted action set

$$\tilde{A}_{(\mathbf{t}, i, s)} := \begin{cases} \hat{A}_{(\mathbf{t}, i-1, s)}, & \text{if } |\hat{A}_{(\mathbf{t}, i-1, s)}| > 0, \\ \{a \mid a = \bar{\pi}_{\text{TLO}}(s', \mathbf{t})\}, & \text{else.} \end{cases} \quad (15)$$

In cases where no actions are known that fulfill the threshold conditions up to objective $i - 1$, and thus $\hat{A}_{(\mathbf{t}, i-1, s)} = \emptyset$, it is assumed that a' is chosen by following the TLO action selection mechanism. As estimations $\mathbf{Q}(s, a, \mathbf{t})_i$ are not used for action selection until $|\hat{A}_{(\mathbf{t}, i-1, s)}| > 0$ (compare (12)), the update in these cases has the purpose to learn the initial expected values until the agent finds a way to fulfill the constraints up to i for state s and action a .

B. Deep gTLO Network

Generalized MORL methods use function approximation to generalize across different preference parameters. In our

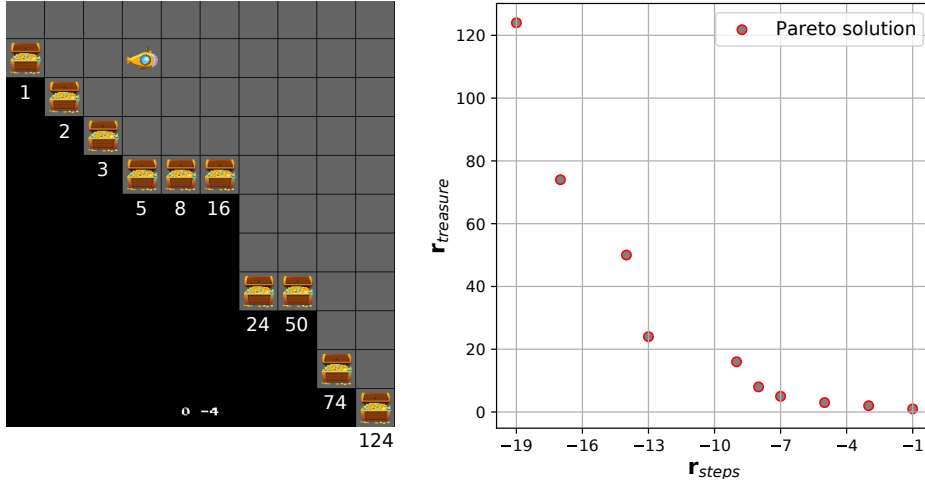


Fig. 3. Deep-sea treasure environment. Left: Screenshot of the DST environment used during evaluation with annotated per treasure rewards. Right: Pareto solutions of the environment in the space of returns.

case, preference parameters are the TLO thresholds \mathbf{t} . We use deep neural networks to approximate the vector-valued multi-objective Q-function $\mathcal{Q}(s, a, \hat{\mathbf{t}}, \theta) \approx \mathcal{Q}(s', a', \hat{\mathbf{t}})$. Vanilla DQN [17] serves as the base algorithm of our *gTLO* implementation. However, we want to emphasize that *gTLO* is compatible with extended DQN versions and other value-based approximate or deep reinforcement learning algorithms.

The extension of a base algorithm for *gTLO* learning is straightforward: The TLO action selection (12) replaces the default greedy policy and for learning, we use an ϵ -greedy version of it. The multi-objective Q-function is approximated by a multi-headed deep neural network \mathcal{Q} as depicted in Fig. 2. The loss-function for \mathcal{Q} is derived from the *gTLO* update defined in (13) to (15).

The *gTLO* network consists of state embedding layers followed by per-objective heads \mathcal{Q}_i . The state embedding layers embed the state s and usually consist either of convolutional layers followed by a flattening layer in the case of image states or fully-connected layers in the case of vector-valued state descriptions. Objective heads \mathcal{Q}_i consist of fully-connected layers and map from state embeddings to \mathcal{Q}_i estimations. While the state embedding is independent of thresholds \mathbf{t} , the \mathcal{Q}_i heads are conditioned on \mathbf{t} . When revisiting the definitions of the action sets $\hat{A}_{(\mathbf{t}, i, s)}$ (11) and $\tilde{A}_{(\mathbf{t}, i, s)}$ (15) underlying the TLO action selection mechanism (12) and the Q-function update (13), one sees that in both cases only thresholds \mathbf{t}_j up to a certain degree are taken into account. In particular, the update and therefore the approximation \mathcal{Q}_i depends on thresholds \mathbf{t}_j with $j < i$. Therefore, it is sufficient to take the vector $\hat{\mathbf{t}}_i = (\mathbf{t}_0, \dots, \mathbf{t}_{i-1})^\top$ into account when learning \mathcal{Q}_i . Expected values for the first objective \mathcal{Q}_0 can be learned without considering \mathbf{t} at all.

The loss for training the *gTLO* network is derived from the TLO bellman update (13). The *gTLO* training target for the experience tuple (s, a, s', \mathbf{r}) and the objective with index i corresponds to the standard DQN target (4):

$$y_{\text{gTLO}, i} := \mathbf{r}_i + \gamma \max_{a' \in \tilde{A}_{(\mathbf{t}, i, s')}} \mathcal{Q}(s', a', \hat{\mathbf{t}}, \theta^-)_i. \quad (16)$$

The per-sample loss is then the sum of per objective losses

$$\mathcal{L}(\theta) := \sum_{i \in [1, I]} \mathcal{H}(y_{\text{gTLO}, i} - \mathcal{Q}(s, a, \hat{\mathbf{t}}, \theta)_i, \delta), \quad (17)$$

where \mathcal{H} is the Huber loss with $\delta = 1$, which was shown to stabilize DQN [17] training.

IV. EXPERIMENTS

A. Deep-Sea Treasure Environment

Deep-sea treasure (DST) [19] is a simple benchmark grid world that is often used to investigate multi-objective reinforcement learning algorithms. In DST, the agent controls a submarine, where the four available actions per step are to move one cell left, right, up and down. When the resulting cell would exceed a grid world border, the submarine's position remains on the current cell. Each episode starts at the upper left cell and ends when the submarine lands on special terminal cells with assigned treasures. The objective of the agent is to maximize the value of treasures collected while using as few steps as possible. The treasure value is reflected by a positive treasure-reward signal $\mathbf{r}_{\text{treasure}}$, which is emitted when a treasure is reached. An efficiency-reward signal $\mathbf{r}_{\text{steps}} = -1$ is emitted in each step.

One of the key features of DST is the possibility to easily define environments with various Pareto front shapes. Our evaluation is based on an image version of the original DST environment [19], which is shown in Fig. 3 (left). It consists of 11×10 cells, with one treasure per column. Treasure values and positions are chosen such that the Pareto front, visualized in Fig 3 (right), is non-convex.

As originally proposed in [18], we use an image version of DST. In the original DST environment, the state is encoded by a one-hot-vector of the submarine's position for investigating tabular MORL methods. In the image version, the state is represented by a down-sampled 84×84 grey-scale image of the current screen output. Our implementation of the environment is based on the *Fruit API* DST implementation [35]. In our implementation, each DST episode ends when a treasure is

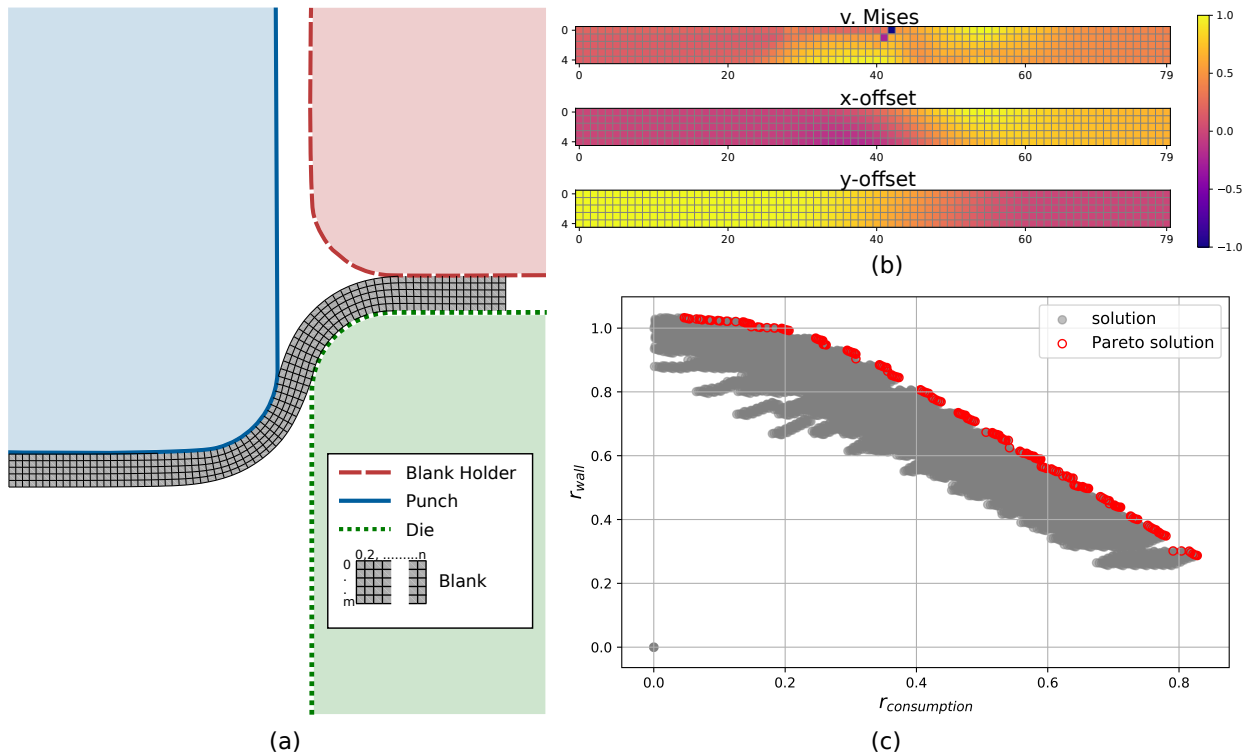


Fig. 4. Deep drawing MORL environment. (a) Components of the rotationally symmetric deep drawing simulation model, where the blank (grey mesh) is drawn by the punch (blue) into the hollow inner part of a die (green), and the blank holder regulates the material flow. (b) Spatially resolved parameters of the blank, as used to describe the process state s . (c) Solutions of the MODP in the space of per-objective returns with Pareto front solutions marked in red.

reached or with a treasure reward of $r_{treasure} = 0$ when 50 time steps have passed.

B. Deep Drawing MORL Environment

To investigate the application of *gTLO* to real-world problems, we use a multi-objective variant of the deep drawing optimal control environment from [29]. A profile view of the deep drawing process is depicted in Fig. 4(a). It is a steel deformation process, where a stamp draws a metal blank into a so-called die to produce a hollow form. Blank holders regulate the material flow. The quality of the process outcome depends to a large extent on the blank holder forces [36]. The online optimization of time-varying blank holder forces regarding the process outcome is the objective of the deep drawing environment. In contrast to the deep-sea treasure environment, the deep drawing process is subject to stochastic conditions in form of a varying friction coefficient. Also, as Fig. 4(c) shows, the amount of policies on the Pareto front is vastly superior when compared to the deep-sea treasure environment.

The deep drawing environment is based on an interactive numerical simulation of the deep drawing process. Each simulated process execution is reflected by an episode of five time steps, in which the process simulation is interrupted and the agent determines the next blank holder force from a discrete action set $A = \{2\text{kN}, 4\text{kN}, 6\text{kN}, 8\text{kN}, 10\text{kN}, 12\text{kN}, 14\text{kN}\}$. At the end of each process execution, a reward is signaled based on a quality assessment of the deep-drawn workpiece. In the multi-objective variant, two conflicting objectives are (a) to reach a leveled wall thickness in the resulting cup and (b)

to minimize the material consumption of the process. These objectives are reflected by a reward vector $\mathbf{r} \in \mathbb{R}^2$. Both reward signals are aggregated from the simulation results as specified in [29]. Instead of the three scalar sensor values which are used in [29] to describe the process state, we assume the observability of stress and geometry data, which we use as state description $\mathbf{s} \in \mathbb{R}^{5 \times 80 \times 3}$. Stress information is given in the form of the von Mises stress in each of the 5×80 elements of the mesh. Geometry information is given by the offset in x - and y -direction regarding the initial positions of the 5×80 blank elements. An exemplary state is visualized in Fig. 4(b). As in the original environment [29], The friction coefficient μ is drawn randomly and independently per episode from a beta distribution with $(\alpha = 1.75, \beta = 5)$, which is rescaled to the range $[0, 0.14]$ and discretized into 10 equally sized bins. Discretization is performed with the purpose of enabling the reuse of previous results of the expensive numerical simulation. Due to the varying process conditions, the optimal policy depends on the friction coefficient. As an exemplary excerpt of the solution space, the set of all solutions with the Pareto front marked in red is visualized in Fig. 4(c) for $\mu = 0.028$, which is the mode of the discretized friction distribution. For a detailed description of the environment and the underlying FEM simulation, we refer to [29].

C. Evaluation Procedure and Metrics

Specific metrics are used to evaluate multi-objective multi-policy methods. The *hypervolume metric* [37] is broadly used in multi-objective optimization to evaluate sets of found

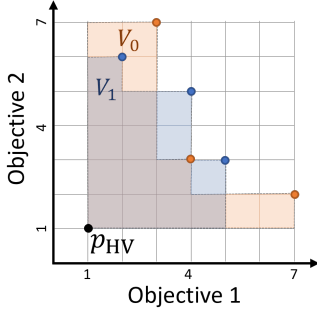


Fig. 5. Hypervolume regions V_0 and V_1 (orange and blue shaded areas) for two solution sets (orange and blue scatters) and the reference point p_{HV} .

solutions. It is defined for a set of solutions and a reference point p_{HV} as the volume of the area between the solutions and p_{HV} and strictly increases with regard to the Pareto dominance relation [26]. For an exemplary two-objective problem, hypervolumes $V_0 = 17$ and $V_1 = 15$ for two exemplary solution-sets, each consisting of three solutions, are depicted in Fig. 5, where each hypervolume equals the allocated shaded area. As proposed in [3] for the case of multi-policy MORL, we use the hypervolume metric as an offline metric, which is periodically calculated during learning. To achieve this, the learning process is interrupted every few learning episodes to perform an evaluation phase. Within the evaluation phase, a solution-set \mathcal{S} is sampled by systematically varying the preferences \mathbf{w} and acting greedily regarding the current state of the Q -function approximations.

If the environment is deterministic and the set of Pareto front solutions \mathcal{P} is finite and known, as it is the case in the deep-sea treasure environment, metrics can be calculated directly based on the solutions found \mathcal{S} and the Pareto solutions \mathcal{P} [12]. For further insight on the deep-sea treasure results, we report the precision (precision = $|\mathcal{S} \cap \mathcal{P}|/|\mathcal{S}|$), the recall (recall = $|\mathcal{S} \cap \mathcal{P}|/|\mathcal{P}|$) and the F1 score

$$F_1 := 2 \times \frac{\text{precision} \times \text{recall}}{\text{precision} + \text{recall}}, \quad (18)$$

as suggested in [12].

For deterministic environments, sampling the policy for a single episode per preference \mathbf{w} is sufficient to calculate the exact offline metrics. In the case of a stochastic environment, however, repeated independent executions are necessary to calculate the statistics of the respective metric. As described in Section IV-B for the deep drawing environment, the probability distribution of the stochastic friction coefficient μ , is discrete and although it is not known to the agent, it can be manually set during the evaluation phase. We take advantage of this by systematically varying the friction coefficient during the evaluation phase and running one evaluation episode for each combination of friction and preference. On this basis, the expected values of evaluation metrics can be calculated also for the deep-drawing environment.

D. Methods and Implementation Details

Methods we considered in the evaluation studies are:

- *gTLO*: our generalized TLO approach as described,
- *gLinear*: generalized MORL based on linear scalarization and a generalized Deep Q-Network
- *dTLQ (outer loop)*: The deep TLQ approach from [25].

To isolate the effect of generalization, we further consider an outer loop variant of our approach which we call *outer loop gTLO*. Using the popular non-linear MORL benchmark deep-sea treasure further allows us to relate our results to previously published results.

The method *gLinear* is based on a scalar, generalized deep Q-network, which is trained to estimate the *expected scalarized return*. It is representative of other linear methods, including current generalized methods, which may converge faster but are also limited to the *convex coverage set*.

gTLO, its variants, and *gLinear* are implemented based on the DQN implementation of the *stable-baselines* framework [38]. The network architecture for the *gTLO* Network as used for the DST experiments is as follows:

- The *state embedding module* $\mathbf{s} \rightarrow \tilde{\mathbf{x}}$ is a slightly altered version of the DQN architecture [17] and consists of three convolution layers with 32, 64, and 64 filters, a filter-size of 8, 4, and 3 and a stride of 4, 2, and 1 followed by a fully-connected layer of 256 neurons.
- The \mathcal{Q}_0 -head $\tilde{\mathbf{x}} \rightarrow (\mathcal{Q}_0(\mathbf{s}, a_0), \mathcal{Q}_0(\mathbf{s}, a_1), \dots, \mathcal{Q}_0(\mathbf{s}, a_n))$ consists of a single fully-connected layer of 128 neurons, followed by the linear output Layer.
- The \mathcal{Q}_1 -head $(\tilde{\mathbf{x}}, \mathbf{t}_0) \rightarrow (\mathcal{Q}_1(\mathbf{s}, a_0), \mathcal{Q}_1(\mathbf{s}, a_1), \dots, \mathcal{Q}_1(\mathbf{s}, a_n))$ consists of two fully-connected layers of 128 and 64 neurons, followed by the linear output Layer.
- The rectified linear unit (ReLU) is used as activation for non-linear layers.

For the deep drawing experiments, we decreased the capacity of the state embedding module, by reducing it to two convolutional layers with 32 and 64 filters. Due to the wide format of the input image (see Fig. 4(b)), filter sizes and strides are reduced to 3 and 1 respectively.

The scalar generalized networks used for the *gLinear* implementation are equal to the *gTLO* state embedding modules followed by a linear output layer.

In general, we train all networks with 8 mini-batches per time step and do not limit the replay-buffer size. We evaluate *dTLQ* based on the implementation as part of the FruitAPI framework of the *dTLQ* author [25], which we extended to enable multiple mini-batches per time step.

For DST, one experiment run consists of 250,000 training time steps with an evaluation phase every 1,000 time steps. For evaluating *gTLO*, the preferences \mathbf{t}_0 are drawn independently per training episode from a set of 100 equidistant values from the interval $[0.5, 100]$. Both environments are two-objective environments, thereby formally, $\mathbf{t}_1 = \infty$ in both cases. Similarly, for evaluating *gLinear*, weights \mathbf{w} are drawn per episode from a set of vectors $\mathbf{w} = \phi(0, 1)^\top + (1-\phi)(1, 0)^\top$ for 100 equidistant values $\phi \in [0, 1]$. For the outer loop algorithms (*dTLQ* and *outer loop gTLO*), preferences \mathbf{t}_0 are drawn from a set of ten preferences, that have been precalculated based on the knowledge of the Pareto front solutions following

[25]: for each pair of each consecutive treasure-values $\mathbf{r}_{\text{treasure}}, \mathbf{r}'_{\text{treasure}}$, including the special case $\mathbf{r}_{\text{treasure}} = 0$, a preference $\mathbf{t}_0 = (\mathbf{r}_{\text{treasure}} + \mathbf{r}'_{\text{treasure}})/2$ is added. The reference point for the hypervolume metric is chosen as $p_{\text{HV}} = (0, -25)$ for DST.

Further DQN parameters for *gTLO* are chosen as follows: the reward is undiscounted ($\gamma = 1$), the target network update frequency used is 5,000 and the warm-up phase lasts 1,000 time steps. For *gLinear*, the discount factor is $\gamma = 0.9$ and the prioritized experience replay is activated with its default parameters ($\alpha_{\text{PER}} = 0.6, \beta_{\text{PER}} = 0.4$).

Each experiment run on the deep drawing environment consists of 12,500 training time steps, where the evaluation phase is conducted every 1,250 time steps. The rewards are scaled to the range $[0, 1]$ based on empirical data and then clipped to ensure $\mathbf{r}_i \in \mathbb{R}_+^2$. The TLO threshold \mathbf{t}_0 is drawn per episode from a set of n equidistant values from the interval $[0, 1.2]$, where for the inner loop (generalized) MORL methods $n = 100$ and for *outer loop gTLO* $n = 10$. The hypervolume reference point is set to $p_{\text{HV}} = (-0.1, -0.1)$. The target networks are updated every 2,505 steps. Other DQN parameters and the preference vectors for *gLinear* are chosen as for the DST experiments.

Code and configurations for reproducing the reported results are published as stated in Section VI-A.

V. RESULTS

A. Deep-Sea Treasure

As described in Section IV-A, an image version of the original DST environment is used to evaluate the MORL methods specified in Section IV-D. The preference is sampled independently per episode from an equal distribution. Per method, ten independent runs of 250,000 training time steps per run are executed. Every 1,000 time steps an evaluation phase is carried out as described in Section IV-C. Evaluation results are visualized in Fig. 6 in form of the mean and 0.95-confidence interval per evaluation phase of the hypervolume metric in Fig. 6(a), the precision in Fig. 6(c), and the recall in Fig. 6(d). Known metric values for the *Pareto coverage set* and the *convex coverage set* are drawn as a black line and dashed black line respectively. In addition, we show the frequency in which each solution from the Pareto front is found within the last evaluation phase of each run per method in Fig. 6(b). The mean and standard deviation of each metric at the end of the 250,000 time steps are listed in Table I for the three methods and the outer loop variant of *gTLO*.

As expected and repeatedly shown in other publications (e.g. [3], [26]) for linear MORL methods, *gLinear* converges to the two extreme solutions which lie on the convex hull of the non-convex Pareto front (compare Fig. 3). *gTLO* manages to repeatedly identify all Pareto front solutions except for rare occurrences (as shown in Fig. 6(b), the solutions with $(2, -3)$ and $(3, -5)$ are not identified in one of the ten runs). The outer loop approach *dTLQ* also covers the whole range of solutions but has problems identifying some individual solutions (at $(3, -5)$ and $(24, -13)$) and rarely identifies the two solutions of highest treasure value. Therefore, *gTLO* clearly outperforms *dTLQ* regarding the recall and the hypervolume metric. While

in the evaluation runs *gLinear* never wrongly determines a dominated policy at the end of learning and achieve a precision-value of 1.0, *gTLO* in rare cases returns policies that are not part of the Pareto front, and thus reaches a mean precision of 0.99.

To investigate the effect of generalization on the sample efficiency of our method, we compare the convergence speed of *gTLO* and the outer loop variant of *gTLO*. The mean amount of steps needed by the outer loop variant until the full Pareto front is found for the first time ($141,555.55 \pm 20,600.97$ steps) is more than double the amount of steps needed by default, inner loop, *gTLO* ($61,000 \pm 20,600.97$ steps). In accordance with already published results for linear generalized methods [9], [10], this shows a positive effect of generalization regarding the sample efficiency also in the non-linear case.

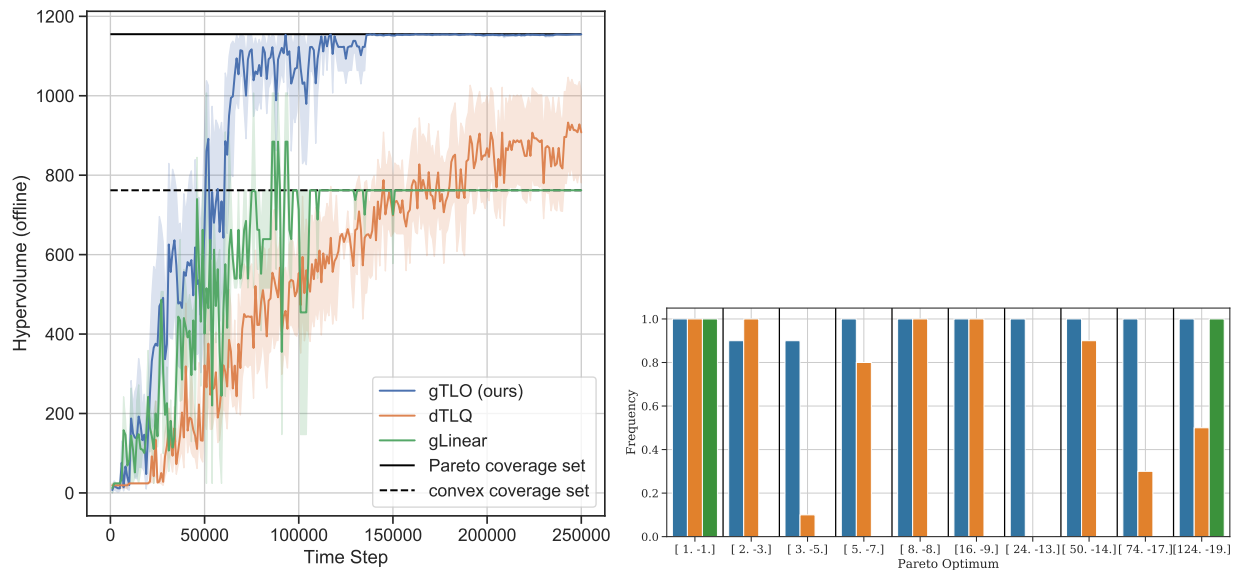
As the deep-sea treasure environment and variants are used for over a decade for evaluating linear and non-linear methods, it is possible to put our results into relation. While often the classical vector version of DST is used, where the state is encoded as one-hot-vector of the submarine’s position [3], [12], [22], [23], [27], some previous deep MORL evaluations are also based on image versions [10], [18], [25]. Evaluations of linear methods [10], [12], [18] are based on convex DST variants. They would converge to the same solution as *gLinear* when applied to the original non-convex DST. The only method that was evaluated on a non-convex image version of DST is *dTLQ* [25], which is shown to solve simplified non-convex DST environments with 3 and 5 treasures after about 300,000 and 1,000,000 total steps respectively.

When it comes to exact, tabular non-linear MORL methods, there are some [3], [22], [23] which completely solve the vector-variant of DST. The steps required until convergence are between 75,000 for TLQ [3], which requires knowledge about the Pareto front, and 1,250,000 steps for MPQ-learning [23]. Other non-linear tabular methods don’t completely solve the problem: Q-learning with a Chebyshev scalarization function converges to a hypervolume of 938.29 [21] and a hypervolume-based inner loop approach reaches 1040.24 [26] of the maximum hypervolume of 1,155.

Pareto DQN [27], the only other inner loop non-linear deep MORL method we identified is evaluated on the one-hot-vector version of DST. In contrast to our work, in [27], details about the Pareto front estimation from the perspective of the first state s_0 are reported instead of agent performance metrics. This prevents a direct comparison of results. Although the general course of the Pareto front is approximated by Pareto DQN, the distribution of the estimated Pareto front solutions differ greatly from the true Pareto front. Furthermore, the estimation quality of PDQN highly depends on the complexity of the state space [27].

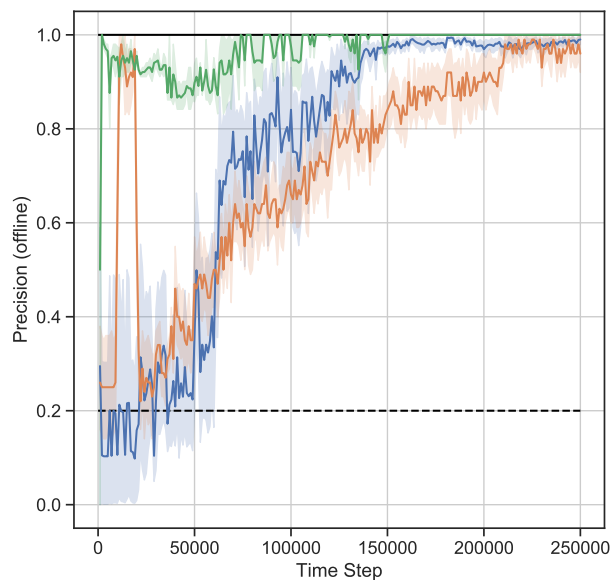
B. Deep Drawing

We evaluate *gTLO*, *gLinear*, and the outer loop variant of *gTLO* on the multi-objective deep drawing environment as it is described in Section IV-B. The evaluation is based on ten independent learning runs per method. As the Pareto front is not known for this environment, ten preferences \mathbf{t}_0 used for *outer loop gTLO* are equally spaced between 0.1 and 1.

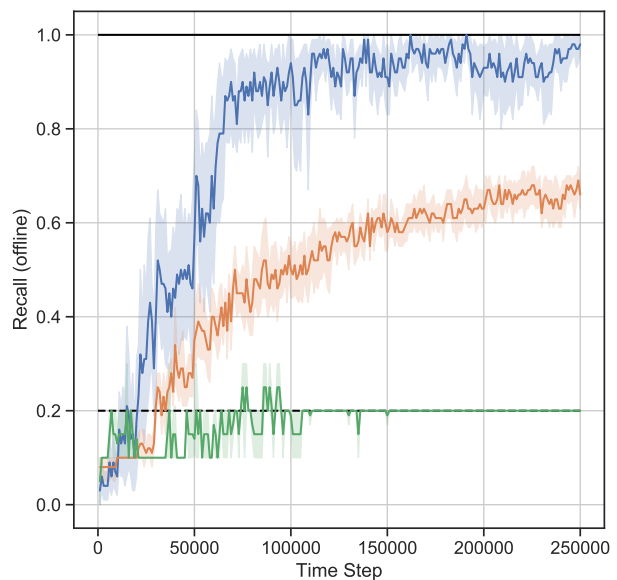


(a) Hypervolume over training time steps per method

(b) Frequency of optimal solutions per method



(c) Precision over training time steps per method



(d) Recall over training time steps per method

Fig. 6. Deep-sea treasure results. (a) Hypervolume metric, (c) precision and (d) recall over time steps per approach. Frequency of determination of each Pareto front solution at the end of learning per approach (b). The hypervolume metric, precision and recall are calculated offline every 1,000 time steps. The mean and the 0.95-confidence interval are plotted per metric and approach. The hypervolume reference is defined as $p_{HV} = (0, -25)$.

In Fig. 7 the mean and the 0.95 confidence interval of the expected hypervolume per evaluation phase is plotted. In early episodes the outer loop variant of *gTLO* is superior. While *gTLO* learns a general state representation, the outer loop variant focuses on one preference per independent model. However, *gTLO* achieves the best quantitative results after approximately 1,250 episodes. *gLinear* is clearly dominated by *gTLO* and its outer loop variant.

Results that allow a more detailed comparison of the three methods are visualized in Fig. 8. In each of the plots, for a combination of method and friction coefficient, attainable solutions are represented by grey dots, and the solution set attained by the respective method is represented by colored

dots. The dot-color hereby encodes the preference value $t_0 \in [0, 1.2]$ for the *gTLO* variants and w as defined in Section IV-D for *gLinear*. For *gTLO*, *outer loop gTLO*, we visualize results from the first of the 10 independent runs, while, due to the slow convergence of *gLinear*, we visualize results of an extended run consisting of 10,000 episodes in this case in Fig. 8(c). Results are visualized for the four most common friction coefficients³ $\mu \in \{0.014, 0.028, 0.042, 0.056\}$.

Fig. 8 reveals, that solutions found by *gTLO* and *outer loop gTLO* cover the reward range very well. As expected, solutions of the linear method are located in the convex

³In over 80% of the episodes one of these is the present friction coefficient (see Section IV-B for details about μ)

TABLE I
RESULTS ON DEEP-SEA TREASURE AFTER 250,000 TRAINING STEPS

| Approach | HVT(0, -25) | Precision | Recall | F1 |
|--------------------------------|---------------------|------------------|--------------------|----------------------|
| gTLO (ours) | 1154.6 ± 0.8 | 0.99 ± 0.015 | 0.98 ± 0.04 | 0.985 ± 0.022 |
| Linear Scalarization | 762.0 ± 0.0 | 1.0 ± 0.0 | 0.2 ± 0.0 | 0.334 ± 0.0 |
| dTLQ (outer loop) ¹ | 907.7 ± 190.61 | 0.96 ± 0.066 | 0.66 ± 0.049 | 0.78 ± 0.044 |
| outer loop gTLO ² | 1150 ± 14.34 | 0.98 ± 0.04 | 0.98 ± 0.04 | 0.98 ± 0.04 |

^aAs implemented in the FruitAPI Framework [25].

^bMerged Single-Policy MORL with gTLO Networks and TLQ Bellman update.

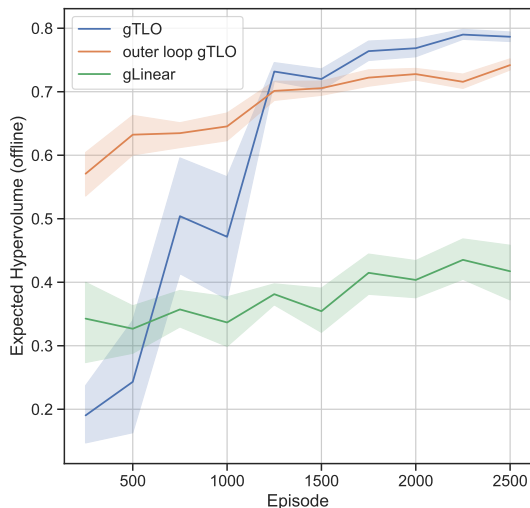


Fig. 7. Expected hypervolumes over episodes ($r_{HV} = (-0.1, -0.1)$) for ten independent runs per method, calculated on evaluation phase results every 500 episodes. The mean value and the 0.95 confidence interval are visualized per method and evaluation phase.

regions near the two ends of the Pareto front, while the middle region of the Pareto front is uncovered. This again shows a major limitation of linear methods in multi-objective reinforcement learning. The gTLO results are in general closer to the per-friction Pareto front. The plot reveals further, that the solutions found by gTLO are much better ordered regarding the preference values than the solutions of the outer loop variant (the hypervolume metric does not take this into account). Different from the deep-sea treasure environment, here the Pareto front can not be fully achieved by the agent due to partial observability.⁴

VI. SUMMARY AND OUTLOOK

In this paper, we introduced generalized Thresholded Lexicographic Ordering (gTLO), a multi-objective deep reinforcement learning algorithm that combines the advantages of generalized MORL and non-linear MORL. Generalized TLO learns multiple preference-dependent policies based on a single deep neural network, thereby transferring process

⁴The agent has no information about the friction coefficient while making the first decision of each episode.

knowledge between different objective preferences and scales to complex MORL problems with a huge set of optimal solutions. Due to the non-linear action selection, gTLO is not limited to solutions from the *convex coverage set*.

To the best of our knowledge, gTLO is the first published generalized non-linear MORL method and is the first method that was shown to solve the image version of the original, non-convex DST benchmark to a very large extent. In the DST study results we highlight that gTLO identifies all solutions from the Pareto front with rare exceptions, and thereby clearly outperforms non-generalizing outer loop methods that relies on the knowledge of positions of the sought solutions in the space of episode returns.

In the studies on our introduced multi-objective deep drawing optimal control environment, we show that gTLO is capable to learn a diverse set of near-optimal solutions also in problems with many Pareto optimal solutions. In direct comparison to the outer loop variant, gTLO provides a set of solutions near the Pareto front that are well-ordered with respect to the preference parameters. For both environments we show empirically that linear MORL methods, as expected, are not capable to identify solutions in non-convex regions of the Pareto front.

Like other TLO-based methods, gTLO is restricted to finite-horizon problems, in which the thresholded reward signals have to be zero during the episode except for the last step [39]. To make the methods applicable to problems with non-zero thresholded rewards during the episode, we think it is promising to resume the early work of Geibel et al. [40] in the context of approximate TLO-based methods such as gTLO.

For evaluation, we implemented gTLO based on vanilla *Deep Q-Networks* (DQN). As it is orthogonal to those DQN extensions, gTLO can be combined with *Double Q-Learning* [41], *Dueling Q-Learning* [42] for more stable learning and *Hindsight Experience Replay* [43] or generalized MORL specific variants thereof such as *Diverse Experience Replay* [10] for sample efficiency.

Other promising opportunities for further development of gTLO include (i) the evaluation on dynamic weight settings with correlated consecutive preference weights [10], (ii) the evaluation on problems with more than two reward terms, and (iii) the extension to partially observed multi-objective Markov decision processes [44], [45].

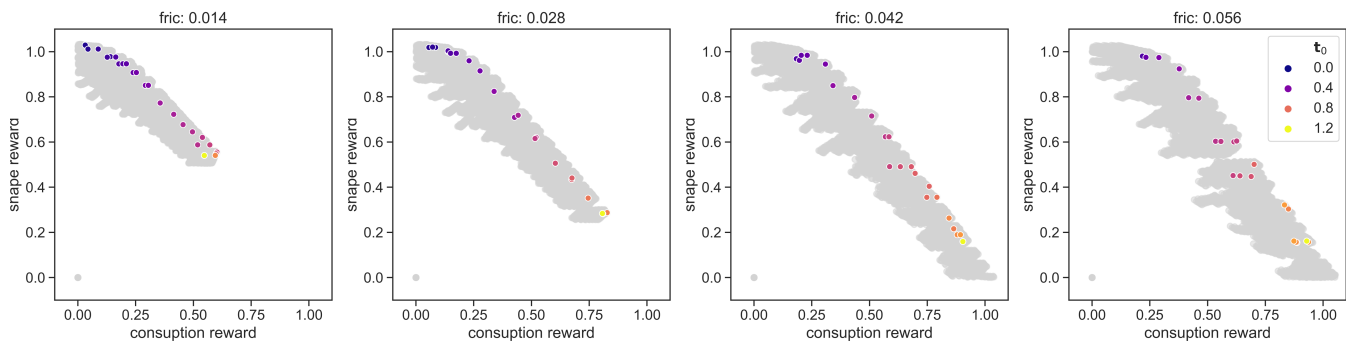
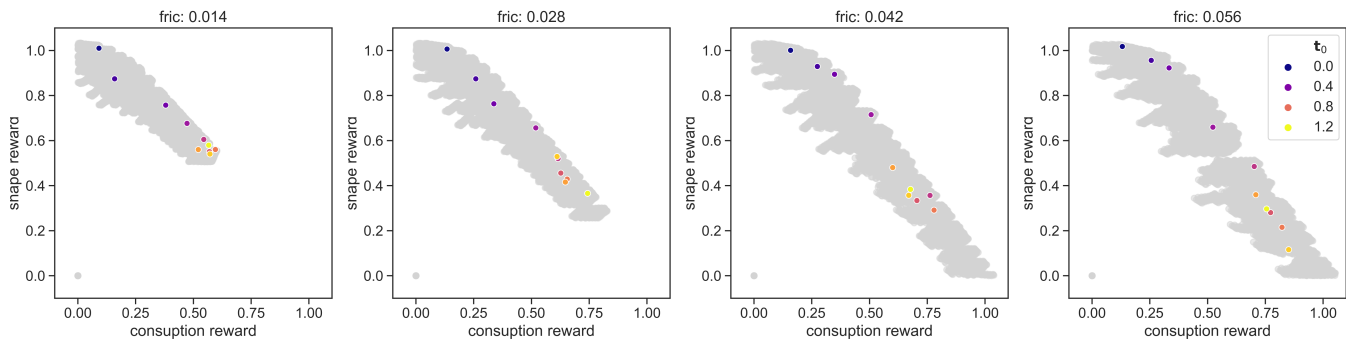
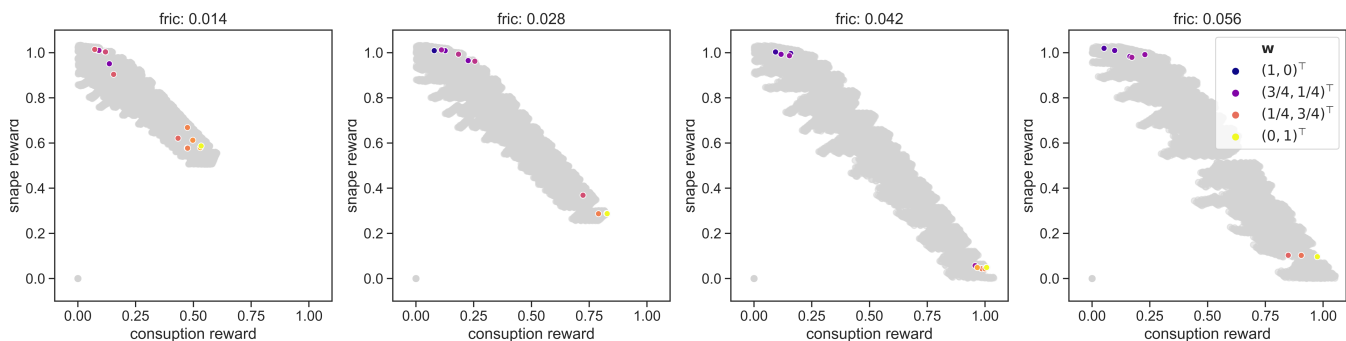
(a) *gTLO* solutions (after 2,500 episodes)(b) *outer loop gTLO* solutions (after 2,500 episodes)(c) *gLinear* solutions (after 10,000 episodes)

Fig. 8. Solutions found by *gTLO*, *outer loop gTLO* and *gLinear* for various friction coefficients μ and preference weights (color coded) after 2,500, 2,500 and 10,000 episodes respectively. For each friction, the attainable returns are visualized as per solution grey dots.

A. Code availability

To simplify reproducibility of our results and subsequent research, we publish the source code of the following modules⁵:

- The implementation of *gTLO* for two-objective environments,
- the deep-sea treasure environment, implemented based on the FruitAPI framework,
- the multi-objective deep drawing environment (requires Abaqus).

⁵<https://github.com/johannes-dornheim/gTLO>

APPENDIX

EQUIVALENCE OF TLO FORMULATIONS

We state that the Thresholded Lexicographic Ordering action selection from Section II-C is equivalent to the policy⁶

$$\bar{\pi}_{\text{TLO}} \leftarrow \begin{cases} \arg \max_{a \in A} \mathbf{Q}(s, a, \mathbf{t})_0, & \text{if } |\hat{A}_{(\mathbf{t}, 0, s)}| = 0, \\ \arg \max_{a \in \hat{A}_{(\mathbf{t}, I, s)}} \mathbf{Q}(s, a, \mathbf{t})_I, & \text{if } |\hat{A}_{(\mathbf{t}, I, s)}| > 0, \\ \arg \max_{a \in \hat{A}_{(\mathbf{t}, i, s)}} \mathbf{Q}(s, a, \mathbf{t})_{i+1}, & \text{otherwise,} \end{cases} \quad (19)$$

where in the third case $i := \max_i : |\hat{A}_{(\mathbf{t}, i, s)}| > 0$. The set $\hat{A}_{(\mathbf{t}, i, s)}$, as defined in (11), stores all actions that are sufficient regarding the expected rewards and thresholds \mathbf{t}_i up to objective i .

From the definition of \hat{A} follows that $\hat{A}_{(\mathbf{t}, i, s)} \subseteq \hat{A}_{(\mathbf{t}, i-1, s)}$ and $|\hat{A}_{(\mathbf{t}, i, s)}| \leq |\hat{A}_{(\mathbf{t}, i-1, s)}|$. Thus, for a given state s and threshold vector \mathbf{t} either all sets $\hat{A}_{(\mathbf{t}, i, s)}$ for $i \in [0, I]$

- (i) are of cardinality 0 (captured by the first case of (19)),
- (ii) contain at least one element (captured by the second case of (19)), or
- (iii) there exists exactly one i for which $|\hat{A}_{(\mathbf{t}, i, s)}| > 0 \wedge |\hat{A}_{(\mathbf{t}, i+1, s)}| = 0$ (captured by the last case in (19)).

From the definitions of $\mathbf{Q}\mathbf{t}$ (8) and $\hat{A}_{(\mathbf{t}, i, s)}$ (11) follows

$$\forall a \in \hat{A}_{(\mathbf{t}, i, s)} : \mathbf{Q}\mathbf{t}(s, a)_i = \mathbf{t}_i, \quad (20)$$

and

$$\forall a \in A \setminus \hat{A}_{(\mathbf{t}, i, s)} : \mathbf{Q}\mathbf{t}(s, a)_i = \mathbf{Q}(s, a)_i. \quad (21)$$

When substituting (21) into (9) for $|\hat{A}_{(\mathbf{t}, 0, s)}| = 0$, it reduces to

$$\sup(a_a, a_b, s, 0) := \mathbf{Q}(s, a_b)_0 > \mathbf{Q}(s, a_a)_0 \vee \text{False} \quad (22)$$

for $a_a, a_b \in A$. This is equivalent to the order relation $\mathbf{Q}(s, a_b)_0 > \mathbf{Q}(s, a_a)_0$, that we use to determine $\pi_{\text{TLO}}(s)$ in the first case of (19).

Next, we assume that there exists an i with $|\hat{A}_{(\mathbf{t}, i, s)}| > 0$. By substituting (20) and (21) into (9) For any $a_a \in \hat{A}_{(\mathbf{t}, i+1, s)}$, $a_b \in \hat{A}_{(\mathbf{t}, i, s)} \setminus \hat{A}_{(\mathbf{t}, i+1, s)}$, we get

$$\sup(a_a, a_b, s, i) := \mathbf{t}_i > \mathbf{t}_i \vee [\mathbf{t}_i = \mathbf{t}_i \wedge (i = I \vee \sup(a_a, a_b, s, i+1))], \quad (23)$$

where

$$\sup(a_a, a_b, s, i+1) := \mathbf{t}_{i+1} > \mathbf{Q}(s, a_b)_{i+1} \vee [\dots] \quad (24)$$

is true. It can be seen that $\sup(a_a, a_b, s, i)$ is fulfilled for any a_a, a_b with $a_a \in \hat{A}_{(\mathbf{t}, i+1, s)}$ and $a_b \in \hat{A}_{(\mathbf{t}, i, s)} \setminus \hat{A}_{(\mathbf{t}, i+1, s)}$. The action π_{TLO} subsequently is either an element of $\hat{A}_{(\mathbf{t}, I, s)}$ if $|\hat{A}_{(\mathbf{t}, I, s)}| > 0$ (the second case in (19))⁷ or an element of

⁶without loss of generality, we ignore the case $Q(s, a_a) = Q(s, a_b)$, for actions $a_a, a_b \in A$, which usually does not occur when function approximation is used.

⁷Mind that $\hat{A}_{(\mathbf{t}, I, s)} = \hat{A}_{(\mathbf{t}, I-1, s)}$, because by definition $t_I := \infty$

$\hat{A}_{(\mathbf{t}, i, s)}$, where $|\hat{A}_{(\mathbf{t}, i, s)}| > 0$ and $|\hat{A}_{(\mathbf{t}, i+1, s)}| = 0$ (the third case of (19)).

For $k = I$ in the case $|\hat{A}_{(\mathbf{t}, I, s)}| > 0$ and $k = i+1$ in the case $|\hat{A}_{(\mathbf{t}, i, s)}| > 0 \wedge |\hat{A}_{(\mathbf{t}, i+1, s)}| = 0$ we now can see, that applying $\sup(a_a, a_b, s, k)$ is equivalent to an ordering of the values in $\hat{A}_{(\mathbf{t}, I, s)}$ and in $\hat{A}_{(\mathbf{t}, i, s)}$ respectively:

$$\sup(a_a, a_b, s, k) := \mathbf{Q}(s, a_b)_k > \mathbf{Q}(s, a_a)_k \vee \text{False}. \quad (25)$$

REFERENCES

- [1] R. S. Sutton and A. G. Barto, *Reinforcement learning: An introduction*. MIT press, 2018.
- [2] D. M. Roijers, P. Vamplew, S. Whiteson, and R. Dazeley, "A survey of multi-objective sequential decision-making," *Journal of Artificial Intelligence Research*, vol. 48, pp. 67–113, 2013.
- [3] P. Vamplew, R. Dazeley, A. Berry, R. Issabekov, and E. Dekker, "Empirical evaluation methods for multiobjective reinforcement learning algorithms," *Machine learning*, vol. 84, no. 1, pp. 51–80, 2011.
- [4] R. Rădulescu, P. Mannion, D. M. Roijers, and A. Nowé, "Multi-objective multi-agent decision making: a utility-based analysis and survey," *Autonomous Agents and Multi-Agent Systems*, vol. 34, no. 1, pp. 1–52, 2020.
- [5] S. Natarajan and P. Tadepalli, "Dynamic preferences in multi-criteria reinforcement learning," in *Proceedings of the 22nd international conference on Machine learning*, 2005, pp. 601–608.
- [6] J. Dornheim and N. Link, "Multiobjective reinforcement learning for reconfigurable adaptive optimal control of manufacturing processes," in *2018 International Symposium on Electronics and Telecommunications (ISETC)*. IEEE, 2018, pp. 1–5.
- [7] D. M. Roijers and S. Whiteson, "Multi-objective decision making," *Synthesis Lectures on Artificial Intelligence and Machine Learning*, vol. 11, no. 1, pp. 1–129, 2017.
- [8] C. F. Hayes, R. Rădulescu, E. Bargiacchi, J. Källström, M. Macfarlane, M. Reymond, T. Verstraeten, L. M. Zintgraf, R. Dazeley, F. Heintz *et al.*, "A practical guide to multi-objective reinforcement learning and planning," *arXiv preprint arXiv:2103.09568*, 2021.
- [9] A. Castelletti, F. Pianosi, and M. Restelli, "Multi-objective fitted q-iteration: Pareto frontier approximation in one single run," in *2011 International Conference on Networking, Sensing and Control*. IEEE, 2011, pp. 260–265.
- [10] A. Abels, D. Roijers, T. Lenaerts, A. Nowé, and D. Steckelmacher, "Dynamic weights in multi-objective deep reinforcement learning," in *International Conference on Machine Learning*. PMLR, 2019, pp. 11–20.
- [11] E. Friedman and F. Fontaine, "Generalizing across multi-objective reward functions in deep reinforcement learning," *arXiv preprint arXiv:1809.06364*, 2018.
- [12] R. Yang, X. Sun, and K. Narasimhan, "A generalized algorithm for multi-objective reinforcement learning and policy adaptation," *Advances in Neural Information Processing Systems*, vol. 32, 2019.
- [13] T. Tajmayer, "Modular multi-objective deep reinforcement learning with decision values," in *2018 Federated conference on computer science and information systems (FedCSIS)*. IEEE, 2018, pp. 85–93.
- [14] D. Ernst, P. Geurts, and L. Wehenkel, "Tree-based batch mode reinforcement learning," *Journal of Machine Learning Research*, vol. 6, pp. 503–556, 2005.
- [15] T. P. Lillicrap, J. J. Hunt, A. Pritzel, N. Heess, T. Erez, Y. Tassa, D. Silver, and D. Wierstra, "Continuous control with deep reinforcement learning," *arXiv preprint arXiv:1509.02971*, 2015.
- [16] M. Andrychpublisherowicz, F. Wolski, A. Ray, J. Schneider, R. Fong, P. Welinder, B. McGrew, J. Tobin, P. Abbeel, and W. Zaremba, "Hindsight Experience Replay," no. Nips, 2017. [Online]. Available: <http://arxiv.org/abs/1707.01495>
- [17] V. Mnih, K. Kavukcuoglu, D. Silver, A. A. Rusu, J. Veness, M. G. Bellemare, A. Graves, M. Riedmiller, A. K. Fidjeland, G. Ostrovski *et al.*, "Human-level control through deep reinforcement learning," *Nature*, vol. 518, no. 7540, p. 529, 2015.
- [18] H. Mossalam, Y. M. Assael, D. M. Roijers, and S. Whiteson, "Multi-objective deep reinforcement learning," *arXiv preprint arXiv:1610.02707*, 2016.

- [19] P. Vamplew, J. Yearwood, R. Dazeley, and A. Berry, "On the limitations of scalarisation for multi-objective reinforcement learning of pareto fronts," in *Australasian joint conference on artificial intelligence*. Springer, 2008, pp. 372–378.
- [20] P. Perny and P. Weng, "On finding compromise solutions in multiobjective markov decision processes," in *ECAI*, vol. 215, 2010, pp. 969–970.
- [21] K. Van Moffaert, M. M. Drugan, and A. Nowé, "Scalarized multi-objective reinforcement learning: Novel design techniques," in *2013 IEEE Symposium on Adaptive Dynamic Programming and Reinforcement Learning (ADPRL)*. IEEE, 2013, pp. 191–199.
- [22] K. Van Moffaert and A. Nowé, "Multi-objective reinforcement learning using sets of pareto dominating policies," *The Journal of Machine Learning Research*, vol. 15, no. 1, pp. 3483–3512, 2014.
- [23] M. Ruiz-Montiel, L. Mandow, and J.-L. Pérez-de-la Cruz, "A temporal difference method for multi-objective reinforcement learning," *Neuro-computing*, vol. 263, pp. 15–25, 2017.
- [24] Z. Gábor, Z. Kalmár, and C. Szepesvári, "Multi-criteria reinforcement learning," in *ICML*, vol. 98. Citeseer, 1998, pp. 197–205.
- [25] T. T. Nguyen, N. D. Nguyen, P. Vamplew, S. Nahavandi, R. Dazeley, and C. P. Lim, "A multi-objective deep reinforcement learning framework," *Engineering Applications of Artificial Intelligence*, vol. 96, p. 103915, 2020.
- [26] K. Van Moffaert, M. M. Drugan, and A. Nowé, "Hypervolume-based multi-objective reinforcement learning," in *International Conference on Evolutionary Multi-Criterion Optimization*. Springer, 2013, pp. 352–366.
- [27] M. Reymond and A. Nowé, "Pareto-dqn: Approximating the pareto front in complex multi-objective decision problems," in *Proceedings of the adaptive and learning agents workshop (ALA-19) at AAMAS*, 2019.
- [28] C. Li and K. Czarniecki, "Urban driving with multi-objective deep reinforcement learning," in *Proceedings of the 18th International Conference on Autonomous Agents and MultiAgent Systems*, 2019, pp. 359–367.
- [29] J. Dornheim, N. Link, and P. Gumbsch, "Model-free adaptive optimal control of episodic fixed-horizon manufacturing processes using reinforcement learning," *International Journal of Control, Automation and Systems*, vol. 18, no. 6, pp. 1593–1604, 2020.
- [30] M. L. Puterman, *Markov decision processes: discrete stochastic dynamic programming*. John Wiley & Sons, 2014.
- [31] C. J. C. H. Watkins, "Learning from delayed rewards," 1989.
- [32] A. Castelletti, G. Corani, A. Rizzolli, R. Soncinie-Sessa, and E. Weber, "Reinforcement learning in the operational management of a water system," in *IFAC workshop on modeling and control in environmental issues*. Citeseer, 2002, pp. 325–330.
- [33] D. M. Roijers, D. Steckelmacher, and A. Nowé, "Multi-objective reinforcement learning for the expected utility of the return," in *Proceedings of the Adaptive and Learning Agents workshop at FAIM*, vol. 2018, 2018.
- [34] N. Sprague and D. Ballard, "Multiple-goal reinforcement learning with modular sarsa (o)," in *Proceedings of the 18th international joint conference on Artificial intelligence*, 2003, pp. 1445–1447.
- [35] N. D. Nguyen, T. T. Nguyen, H. Nguyen, D. Creighton, and S. Nahavandi, "Review, analysis and design of a comprehensive deep reinforcement learning framework," *arXiv preprint arXiv:2002.11883*, 2020.
- [36] C. P. Singh and G. Agnihotri, "Study of deep drawing process parameters: a review," *International Journal of Scientific and Research Publications*, vol. 5, no. 2, pp. 1–15, 2015.
- [37] E. Zitzler, L. Thiele, M. Laumanns, C. M. Fonseca, and V. G. Da Fonseca, "Performance assessment of multiobjective optimizers: An analysis and review," *IEEE Transactions on evolutionary computation*, vol. 7, no. 2, pp. 117–132, 2003.
- [38] A. Hill, A. Raffin, M. Ernestus, A. Gleave, A. Kanervisto, R. Traore, P. Dhariwal, C. Hesse, O. Klimov, A. Nichol, M. Plappert, A. Radford, J. Schulman, S. Sidor, and Y. Wu, "Stable baselines," <https://github.com/hill-a/stable-baselines>, 2018.
- [39] R. Issabekov and P. Vamplew, "An empirical comparison of two common multiobjective reinforcement learning algorithms," in *Australasian Joint Conference on Artificial Intelligence*. Springer, 2012, pp. 626–636.
- [40] P. Geibel, "Reinforcement learning for mdps with constraints," in *European Conference on Machine Learning*. Springer, 2006, pp. 646–653.
- [41] H. Van Hasselt, A. Guez, and D. Silver, "Deep reinforcement learning with double q-learning," in *Proceedings of the AAAI conference on artificial intelligence*, vol. 30, no. 1, 2016.
- [42] Z. Wang, T. Schaul, M. Hessel, H. Hasselt, M. Lanctot, and N. Freitas, "Dueling network architectures for deep reinforcement learning," in *International conference on machine learning*. PMLR, 2016, pp. 1995–2003.
- [43] T. Schaul, J. Quan, I. Antonoglou, and D. Silver, "Prioritized experience replay," *arXiv preprint arXiv:1511.05952*, 2015.
- [44] D. M. Roijers, S. Whiteson, and F. A. Oliehoek, "Point-based planning for multi-objective pomdps," in *Twenty-Fourth International Joint Conference on Artificial Intelligence*, 2015.
- [45] K. H. Wray and S. Zilberstein, "Multi-objective pomdps with lexicographic reward preferences," in *Twenty-Fourth International Joint Conference on Artificial Intelligence*, 2015.